

High-resolution seismic tomography across the 1980 (Ms 6.9) Southern Italy earthquake fault scarp

Luigi Improta and Aldo Zollo

Department of Physics, University of Naples, Naples, Italy

Pier Paolo Bruno and Andre Herrero

Istituto Nazionale di Geofisica e Vulcanologia, Italy

Fabio Villani

Department of Earth Science, University of Naples, Naples, Italy

Received 7 February 2003; revised 3 April 2003; accepted 8 April 2003; published 16 May 2003.

[1] A high-resolution multi-fold wide-angle seismic survey carried out across the Irpinia fault, Southern Italy, yields new information about the shallow structure of this normal fault that was reactivated in 1980. The fault zone is imaged to a depth of about 60 m by using a non-linear tomographic technique that is specially designed to image strongly heterogeneous media. Results confirm the location of the fault, as previously inferred by a trench excavated in soft soils, and clearly delineates a 30–35 m step in the bedrock. This single step is indicative of a narrow fault zone, which corresponds upward to warped soils exposed in the trench, thus demonstrating that the near-surface warping is directly related to a brittle faulting in the bedrock. Assuming that the vertical slip rate yielded by paleoseismic data (0.25–0.35 mm/yr) has been constant since the fault's inception, the latter should date back to about 100–140 kys ago. Such a young age may explain why the Irpinia fault is not associated with evident, large-scale geomorphic indicators of its activity. **INDEX TERMS:** 0902 Exploration Geophysics: Computational methods, seismic; 7221 Seismology: Paleoseismology; 7223 Seismology: Seismic hazard assessment and prediction; 8010 Structural Geology: Fractures and faults; 8180 Tectonophysics: Tomography. **Citation:** Improta, L., A. Zollo, P. P. Bruno, A. Herrero, and F. Villani, High-resolution seismic tomography across the 1980 (Ms 6.9) Southern Italy earthquake fault scarp, *Geophys. Res. Lett.*, 30(10), 1494, doi:10.1029/2003GL017077, 2003.

1. Introduction

[2] The Southern Apennine seismic belt (Italy), with up to $M = 7.1$ earthquakes, is one of the most active seismic areas in the Mediterranean region. The belt extends NW-SE along the axis of the Apennine range, and is characterized by a NE-oriented extension stress regime, as clearly testified by predominant NW-trending normal-faulting mechanisms [Amato and Montone, 1997]. This stress regime has been active since 700 kyr and follows the Miocene-Lower Pleistocene compressive tectonics responsible for the growth of the Apennine range. Due to the youthfulness of the tectonic regime change, and to low extension rates (1–3 mm/yr, according to Jackson and McKenzie [1988]),

in the axial zone of the range the landscape is still dominated by geomorphic features inherited from the compressive tectonics. On the contrary, the recent normal-faulting activity is associated with only subtle geomorphic expressions, such as remains of fault scarps escaped from the intense erosion processes of the region and small intermontane basins, which are indicative of small cumulative displacements along the faults [Pantosti and Valensise, 1990]. This makes challenging the identification of active faults either by geomorphic mapping or conventional seismic exploration, and allows to explain why most of the large Apennine historical earthquakes have not been associated with precise causative faults so far. The Irpinia Fault (IF), the causative fault of the disastrous (more than 3000 casualties) 1980 Southern Italy earthquake, is a clear proof of these difficulties. It has been recognized solely after the 1980 event on the basis of an extensive fault scarp, which does not match any previously mapped fault in the region, lacking clear geomorphic manifestations of recent faulting activity prior the earthquake [Pantosti and Valensise, 1990].

[3] In such a context, high-resolution seismic exploration can provide valuable information for identifying near-surface recent faulting. Conventional high-resolution reflection seismic has been used successfully to reveal the shallow geometry of major active faults in western US [e.g., Dolan and Pratt, 1997]. However, seismic imaging of near-surface faulting in unconsolidated sediments is often hampered by diffraction/scattering phenomena, strong multiples and static problems in the data, which are caused by small-scale heterogeneities and strong velocity variations in the shallow soils and in the fault zone. Moreover, in presence of strong lateral velocity changes, standard velocity analysis are inappropriate to estimate a reliable background model, which is a key element for the successful application of standard migration techniques. To overcome these limitations, Morey and Schuster [1999] recently proposed the use of high-resolution seismic tomography as alternative mean to image near-surface fault systems.

[4] In this paper we apply a new non-linear tomographic technique to dense seismic data collected with a multi-fold wide-angle geometry across the IF. The main goals of this study were (1) to investigate whether the acquisition and inversion procedures used, which are especially designed to image strongly heterogeneous media, may be effective tools to identify a fault zone in unconsolidated sediments; (2) to

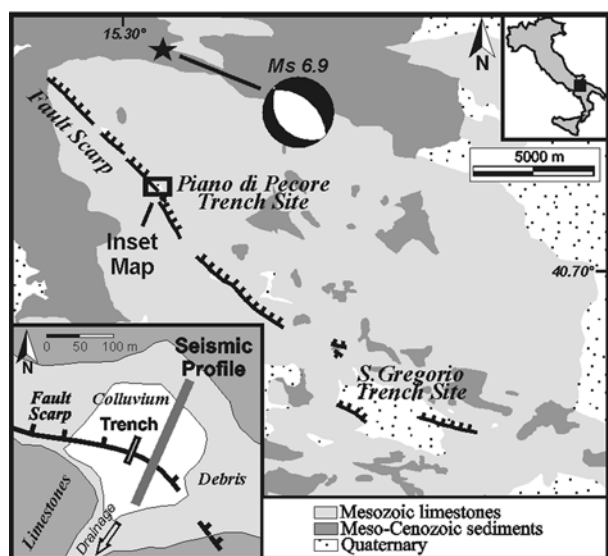


Figure 1. Map of the 1980 Irpinia fault surface breakage along the central and southern strands [modified after *Pantosti and Valensise, 1990*]. The epicenter (star) and focal mechanism of the 1980 earthquake are also shown. Inset map shows locations of the seismic profile and trench in the Piano di Pecore basin.

obtain new information about the near-surface structure of the IF. As test site we selected a small intermontane basin, such a structure often representing the only, subtle geomorphic indicator of recent faulting activity in the Southern Apennine.

2. The Seismic Survey

[5] The IF is a NE-dipping normal fault, which extends NW-SE along the axial zone of the Campania-Lucania Apennine. This fault was reactivated in the 1980, Ms 6.9, Southern Italy earthquake, which produced a fault scarp along three main strands for a total length of 38 km [*Pantosti and Valensise, 1990*]. Trenches opened by *Pantosti et al. [1993]* and *D'Addezio et al. [1991]* across the fault scarp in two Quaternary basins, about 25 km apart (Figure 1), exposed the geologic records of at least four Holocene paleoearthquakes. The authors interpret the 1980 earthquake as a *characteristic event* for the IF [*Schwartz and Copper-smith, 1984*], based on a good agreement between the timing of the earthquakes recognized in the different trench sites, on the similar deformation style and on the repeated amount of slip among the events. Based on scant stratigraphic field data, *Pantosti et al. [1993]* set the upper bound for the total vertical slip along the fault at 350 m.

[6] In 1999 we conducted a high-resolution seismic survey across the central strand of the IF at the Piano di Pecore trench site [*Pantosti et al., 1993*] (Figure 1). The Piano di Pecore is a small intermontane basin emplaced on Mesozoic limestones and filled by Quaternary deposits. In 1980 the fault produced a surface warping about 15-m-wide and 0.5-m-deep in the central part of the basin. The fault acts like a damming structure, lowering the northern sector of the basin and breaking off the natural drainage that flows southward across the basin. A 4-m-deep trench excavated in soft soils exposed evidence of four earthquakes occurred in the last 8600 yr, for a total vertical slip of 3 m. Each event caused a

warping deformation in the soils and a new sequence of lacustrine deposits and scarp-derived colluvium, which ponded behind the fault scarp filling the fault hanging wall.

[7] We collected a 200-m-long seismic profile subparallel to, and offset about 20 m from, the trench in order to investigate the basin structure and the fault zone for depths below those reached by trenching (Figure 1). The acquisition layout consisted of an array of 24, 14 Hz, receivers deployed with a 10 m interval at the basin edge and with a 5 m interval in the fault zone. The receivers recorded 234 shots fired with a spacing of 0.5 in the fault zone and of 1 m along the profile sides. Being interested in high-resolution seismic tomography (HRST), we used this multi-fold wide-angle geometry since it allows to collect highly redundant turning waves and deep-penetrating refracted waves, which contain information on the velocity distribution in depth.

[8] All record sections exhibit clear first arrivals, even at large offsets, which allow an accurate picking. Secondary arrivals are instead affected by diffraction/scattering phenomena and strong surface waves (Figure 2). First arrivals were handpicked from 5195 traces with uncertainties ranging from 4 ms (1/4 of the dominant period) to 20 ms.

3. The High Resolution Seismic Tomography

[9] Due to the presence of unconsolidated sediments overlying an irregular limestone basement, we expect severe velocity variations in the basin, too strong for a linear inverse problem to be formulated. In addition, no *a priori* information about the basin structure (i.e. a reliable reference model) is available. Thus, we used a non-linear tomographic technique, recently proposed by *Herrero et al. [2000]*, which is especially designed to image strongly heterogeneous media. Traveltimes are computed by a finite-difference Eikonal solver [*Podvin and Lecomte, 1991*]. The model is parameterized by a bi-cubic spline interpolation of a regular grid of velocity nodes. The inversion procedure combines a multi-scale approach and a non-linear optimization scheme. A succession of inversions is run by progressively thickening the velocity grid, and for each inversion run the minimum cost function model is found by a combined global/local search [details on the method can be found in *Improta et al., 2002*].

[10] For the Piano di Pecore data, the inversion procedure consists of a succession of five inversion runs. The final 100-node model (Figure 3) shows a rms traveltimes residual of 7 ms, which is slightly higher than the average picking

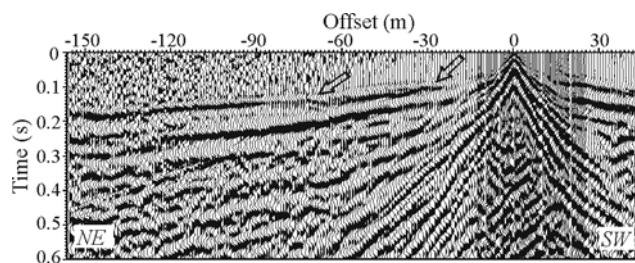


Figure 2. Example of Common Receiver Gather panel. The arrows outline two knee joints in the first-arrival traveltimes curves. Note the clear first arrivals. Near-vertical secondary arrivals are instead dominated by ground roll and strong diffractions.

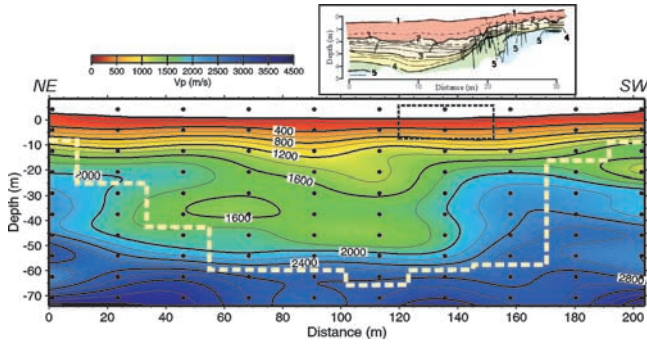


Figure 3. The final tomographic image parameterized by 100 nodes (black circles). The dashed line bounds the best resolved region of the model. The dashed box corresponds to the schematic drawing of the trench showed above [after Pantosti *et al.*, 1993]; each heavy line labeled with a number corresponds to the ground surface at the time of a paleoearthquake.

error (6 ms). Model resolution is assessed by *a posteriori* checkerboard tests [Improta *et al.*, 2002]. The best resolved region extends up to 60–65 m depth in the 50–170 m distance range (Figure 4a).

[11] Figure 3 shows a quite complex velocity field, with regions of high vertical gradient and important lateral changes. The near-surface structure is characterised by very low velocity values (200–400 m/s) and by isovelocity lines gently rising on the model sides. In the 5–10 m depth range a shallow region of high vertical gradient causes a rapid velocity increase from 400 to 1200–1400 m/s. North of the surface fault expression, this region shows an arched shape, with the deflection of the isovelocity contours that is progressively larger for increasing velocities. At greater depths the model shows two distinct sections separated by a strong lateral velocity variation located beneath the trench site. To

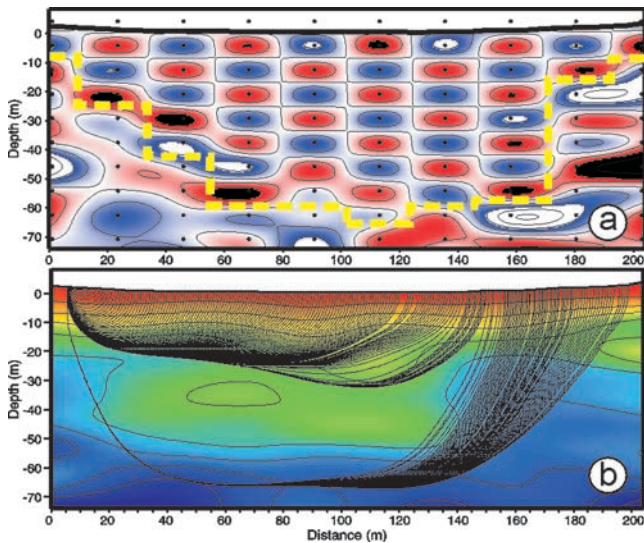


Figure 4. (a) Perturbation pattern retrieved after the *a posteriori* checkerboard resolution test. The perturbation is a 10×10 cell pattern with a maximum value of ± 30 m/s. The dashed line bounds the best resolved region of the model. (b) Example of first arrivals back ray-tracing in the velocity model.

the north, in the 20–50 m depth interval, the velocity ranges from 1600 to 1800 m/s and the contours dip southward. The 50–60 m depth range corresponds to a region of high vertical velocity gradient with a sharp increase from 1800 to 2400 m/s. To the south, this high gradient region is shallower and a sharp velocity increase from 1800 to 2200 m/s occurs in the 20–25 depth range. This results in an abrupt change in depth of the isovelocity lines beneath the trench, which is evident for the 1800–2200 m/s contours showing a vertical separation of 30–35 m.

4. Discussion

[12] The two regions of high vertical gradient suggest the presence of strong discontinuities. A few lines of evidence support this interpretation. (1) Two clear knee joints are present in the first-arrival traveltimes curve at about 30 and 80 m offset for all record sections (Figure 2). (2) Ray maps obtained by a back ray-tracing procedure [Podvin and Lecomte, 1991] show within the high gradient regions paths that bear a remarkable resemblance to head-waves (Figure 4b). (3) To complement information from the HRST, we obtained a reflectivity image by common depth point processing of the seismic data. Taking advantage of the HRST, we used the tomographic model for both normal moveout and static corrections. Indeed, in presence of strong lateral velocity changes, the use of a tomographic velocity model yields a better stacking for near-surface reflections than other methods, and improves also the time-to-depth conversion [Miller *et al.*, 1998]. Although the reflectivity image does not reveal the basin shallow structure mainly because of poor data quality up to 50 ms, prominent reflections are evident in the central part of the section from 50 to 60 m depth, this depth range corresponding to the region of high vertical gradient (Figure 5). Further, there are hints between CMPs 300 and 350 of reflection truncations that are indicative of normal-faulting.

[13] From the combined high-resolution tomographic and reflectivity images, we interpreted the lower region of high vertical gradient as the top of the carbonate bedrock (Figure 6). Indeed, the high velocities (2000–2800 m/s) found in lower region of the model pertain to the bedrock consisting of weathered, fractured limestones which crop out in the surrounding mountains [Guadagno and Nunziata, 1993].

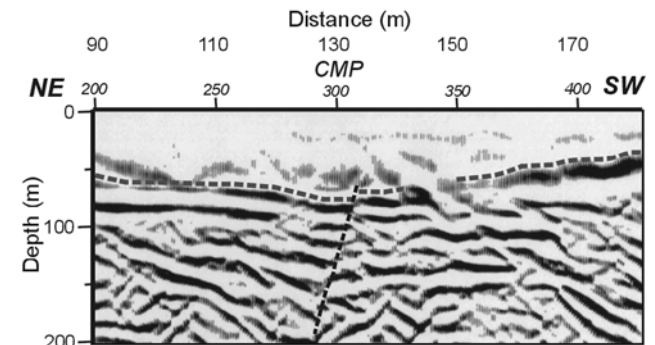


Figure 5. The post-stack depth converted section obtained by common depth point processing. Although the shallow structure of the basin is not imaged, the strong events in the 50–60 m depth range are indicative of the carbonate bedrock.

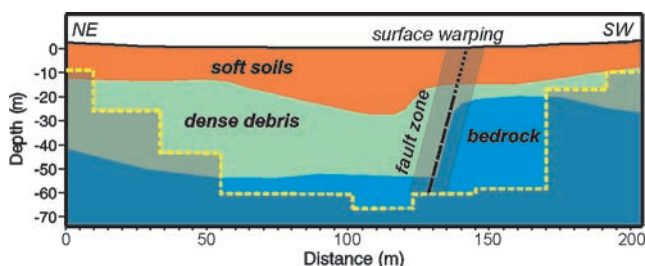


Figure 6. Schematic geological interpretation of the tomographic image.

The sudden change in depth of the 1800–2200 isovelocity lines can be thus interpreted as a step in the limestones caused by the IF, with the bedrock 30–35 m deeper in the hanging wall than in the footwall. The shallow discontinuity is interpreted to separate near-surface colluvial and lacustrine soft deposits from dense coarse deposits, mainly consisting of carbonate debris, which are exposed at the basin edges. Some features in the upper part of the model can be interpreted as further indicators of fault activity. The deflection of the isovelocity lines north of the fault surface expression is in agreement with the expected thickening of the soft soils, which ponded behind the fault. Moreover, the increase of the deflection with depth may be related to a cumulative warping caused by repeated earthquakes, as shown by trench data (Figure 3). The progressive filling of the fault hanging wall allows to explain the abrupt thickening of the intermediate layer (dense debris), while its southward dipping is consistent with tilting of shallow strata, as commonly observed for normal-fault structures.

[14] The velocity image confirms therefore the fault location, as inferred by geomorphic and trench data, and reveals new geologic features below the trench. It suggests that displacement concentrates in a narrow zone, corresponding to the step in the carbonate substratum, while no further large fault splays are present in the central part of the basin, outside the sector investigated by the trench. This demonstrates that the near-surface warping deformation found by *Pantosti et al.* [1993] trenching soft soils is directly related to a concentrated brittle normal-faulting in the underlying limestones.

[15] A noticeable result is the small amount (30–35 m) of total vertical slip separation imaged for the carbonate bedrock across the IF. This result is consistent with new geomorphic data collected in a 250 km² wide area surrounding the Piano di Pecore site [*Ascione et al.*, 2003]. The authors set 50 m as the upper bound for the IF total throw, based on the relationships between Late Pliocene-Early Pleistocene relic erosional surfaces and all the few Pleistocene fault scarps in the study area. The lack of large cumulative slip is also suggested by a crustal reflection profile across the IF southern strand [*Mazzotti et al.*, 2000], which does not reveal the fault at crustal depth, thus suggesting that its total throw is not large enough to be imaged by conventional reflection seismic.

[16] Combining paleoseismic data with the 30–35 m of total vertical slip inferred by tomography, we speculatively estimate the age of the fault inception. Assuming that the 0.25–0.35 mm/yr vertical slip rate estimated by *Pantosti et al.* [1993] is representative of the entire IF history, we

obtain that the fault activity in the Piano di Pecore area started about 100–140 kys ago.

[17] Ultimately, this study reveals the advantages of using HRST in conjunction with geomorphic mapping and paleoseismology for singling out surface faulting, and analyzing shallow fault zones for depths below those reached by trenching. This is evident in the Southern Apennine range, where in the absence of clear geomorphic indicators of recent surface faulting, HRST can be an effective and cheap tool for locating optimal trench sites. Furthermore, in mountainous regions as the Apennine range, where trench excavation is often impractical because of the poor accessibility to potential sites, HRST can be a viable, substitutive technique to investigate shallow fault zones.

[18] **Acknowledgments.** We thank Prof. R. Scarpa and an anonymous reviewer for comments on the manuscript and C. Piromallo for the English reviewing. This study is funded by GNDT and MIUR through the program CIPE-MURST.

References

- Amato, A., and P. Montone, Present day stress field and active tectonics in southern peninsular Italy, *Geophys. J. Int.*, 130, 519–534, 1997.
- Ascione, S., A. Cinque, L. Improta, and F. Villani, Late quaternary faulting within the Southern Apennines seismic belt: New data from the Mt. Marzano area (Southern Italy), *Quaternary Int.*, 99–101–102, 27–41, 2003.
- D’Addezio, G., D. Pantosti, and G. Valensise, Paleoseismicity along the Irpinia fault at the Pantano di San Gregorio Magno (southern Italy), *Quaternario*, 4(1a), 121–136, 1991.
- Dolan, J. F., and T. L. Pratt, High resolution seismic reflection profiling of the Santa Monica fault zone, West Los Angeles, California, *Geophys. Res. Lett.*, 24(16), 2051–2054, 1997.
- Guadagno, F. M., and C. Nunziata, Seismic velocity of fractured carbonate rocks (Southern Apennines Italy), *Geophys. J. Int.*, 113, 739–746, 1993.
- Herrero, A., L. Improta, A. Zollo, P. Dell’Aversana, and S. Morandi, 2-D Nonlinear traveltimes tomography by multi-scale search: Imaging an overthrust structure in the Southern Apennines, *AGU 2000 Fall Meeting, Eos Trans. AGU*, 81, 418, 910, 2000.
- Improta, L., A. Zollo, A. Herrero, M. R. Frattini, J. Virieux, and P. Dell’Aversana, Seismic imaging of complex structures by non-linear traveltimes inversion of dense wide-angle data: Application to a thrust belt, *Geophys. J. Int.*, 151, 264–278, 2002.
- Jackson, J. A., and D. P. McKenzie, The relationship between plate motions and seismic moment tensor, and the rates of active deformation in the Mediterranean and Middle East, *Geophys. J.*, 93, 45–73, 1988.
- Mazzotti, A. P., E. Stucchi, G. L. Fradelizio, L. Zanzi, and P. Scandone, Seismic exploration in complex terrains: A processing experience in the Southern Apennines, *Geophysics*, 65(5), 1402–1417, 2000.
- Miller, K. C., S. H. Harder, D. C. Adams, and T. O’Donnell, Integrating high-resolution refraction data into near-surface seismic reflection data processing and interpretation, *Geophysics*, 63, 1339–1347, 1998.
- Morey, D., and G. T. Schuster, Paleoseismicity of the Oquirrh fault, Utah, from shallow seismic tomography, *Geophys. J. Int.*, 138, 25–35, 1999.
- Pantosti, D., and G. Valensise, Faulting mechanism and complexity of the November 23, 1980, Campania-Lucania earthquake, inferred from surface observations, *J. Geophys. Res.*, 95(15), 319–341, 1990.
- Pantosti, D., D. P. Schwartz, and G. Valensise, Paleoseismology along the 1980 surface rupture of the Irpinia fault: Implications for earthquake recurrence in the Southern Apennines, Italy, *J. Geophys. Res.*, 98(B4), 6561–6577, 1993.
- Podvin, P., and I. Lecomte, Finite difference computation of traveltimes in very contrasted velocity model: A massively parallel approach and its associated tools, *Geophys. J. Int.*, 105, 271–284, 1991.
- Schwartz, D. P., and K. J. Coppersmith, Fault behavior and characteristic earthquake: Examples from the Wasatch and San Andreas fault zones, *J. Geophys. Res.*, 89, 5681–5698, 1984.

L. Improta and A. Zollo, Department of Physics, University of Naples, Via Cintia, 80126, Naples, Italy. (improta@na.infn.it; zollo@na.infn.it)

P. P. Bruno, INGV, Osservatorio Vesuviano, Via Diocleziano 328, 80124 Naples, Italy.

A. Herrero, INGV, Via di Vigna Murata 605, 00143, Rome, Italy.

F. Villani, Department of Earth Science, University of Naples, Largo S. Marcellino 10, 80138, Naples, Italy.